RSC Advances

Cite this: *RSC Advances*, 2011, **1**, 187–190

www.rsc.org/advances

COMMUNICATION

One-pot alkaline vapor oxidation synthesis and electrocatalytic activity towards glucose oxidation of CuO nanobelt arrays†

Tetsuro Soejima,*[ab] Hitomi Yagyu,[a] Nobuo Kimizuka[bc] and Seishiro Ito[a]

Received 26th April 2011, Accepted 24th June 2011
DOI: 10.1039/c1ra00109d

CuO nanobelt arrays supported on copper substrates are synthesized by a simple and one-pot low-temperature vapor oxidation method. The CuO nanobelt arrays show high electrocatalytic activity towards glucose oxidation.

Cupric oxide (CuO) compounds have recently received significant attention due their application in important devices, including high-temperature semiconductors[1] and magnetic storage media.[2] CuO is a p-type semiconducting material (E_g = 1.2 eV) that exhibits field emission,[3] photovoltaic,[4] photoconductive,[5] and gas-sensing properties.[6] Due to its photochemical and (photo)conductive properties, CuO has been exploited for photocatalysts,[7] solar cells,[8] and lithium ion batteries.[9] Additionally, CuO materials facilitate the catalysis of many reactions including cross-couplings,[10] CO and NO oxidation,[11] propylene oxidation to acrolein,[12] and olefin epoxidation.[13]

Recently, arrayed one- or two-dimensional nanocrystals (nanowires, nanosheets, nanobelts), nanoarrays, have attracted considerable interest[14] because of their potential for a variety of different applications, such as nanolasers,[15] dye-sensitized solar cells,[16] lithium ion batteries,[17] nano-generators,[18] unique adhesive nanomaterials,[19] and optical sensors.[20] The design and fabrication of nanoarrays is essential for the creation of smart, high-performance nanodevices. To date, CuO nanoarrays have been prepared by several methods. For instance, CuO nanoribbons were obtained by the heat treatment of $Cu(OH)_2$ nanoribbons at 180 °C with a constant flow of N_2.[21] Xia *et al.* reported the high-temperature (500 °C) synthesis of CuO nanowires supported on the surfaces of various copper substrates including grids, foils, and wires.[22] Thus, relatively high-temperatures and/or a controlled atmosphere are necessary to form CuO crystals in the gas-phase. CuO nanoarray structures have also been formed at low temperatures (<60 °C) in alkaline aqueous solutions. However, the liquid-phase synthetic methods require a long reaction time (>20 h) to form complete CuO nanoarrays.[23–24]

In this paper, we report a novel one-pot and low-temperature synthetic route to CuO nanobelt arrays on a Cu substrate. The simple growth approach *via* alkaline vapor oxidation (VO, Fig. S1†)[25] under mild and facile conditions makes it possible to rapidly fabricate CuO nanobelts compared with those of liquid-phase synthetic methods. Additionally, CuO/ZnO composite nanoarrays can be obtained utilizing the VO process. The CuO nanobelt arrays/Cu electrode shows excellent oxidation of glucose in a basic solution and high sensitivity as a nonenzymatic glucose sensor.

To synthesize the nanobelt arrays, a copper plate was half immersed in an aqueous solution of 100 mM NH_3–100 mM H_2O_2 at an angle against the wall of a glass vial (Fig. 1A) and kept at 80 °C

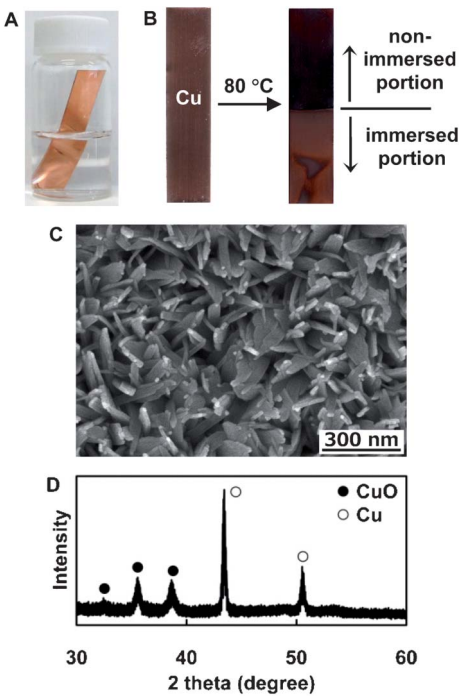

Fig. 1 (A) A picture of the screw vial containing NH_3–H_2O_2 aqueous solution and an immersed Cu substrate during the reaction. (B) Pictures of the Cu plate before (left) and after (right) the reaction. An SEM image (C) and XRD pattern (D) of CuO nanobelt arrays formed on the non-immersed portion of the Cu plate by the VO reaction.

[a]*Department of Applied Chemistry, School of Science and Engineering, Kinki University, 3-4-1 Kowakae, Higashi-osaka, Osaka, 577-8502, Japan. E-mail: soejima@apch.kindai.ac.jp; Fax: +81-6-6721-2024; Tel: +81-6-6721-2332*
[b]*CREST, Japan Science and Technology Agency, 744 Moto-oka, Nishi-ku, Fukuoka, 819-0395, Japan*
[c]*Department of Chemistry and Biochemistry, Graduate School of Engineering, Kyushu University, 744 Moto-oka, Nishi-ku, Fukuoka, 819-0395, Japan*

† Electronic supplementary information (ESI) available: Explanation of the VO process. SEM images and XRD patterns of Cu or brass plates after the VO reaction. CV data for the CuO nanobelt arrays/Cu electrode. See DOI: 10.1039/c1ra00109d

for 7 h in a laboratory drying oven. The sample was then washed with distilled water and dried in air at room temperature. Fig. 1B shows the changes in the appearance of the Cu plate before and after the reaction. There was no significant change in the color of the portion that was immersed in the NH_3–H_2O_2 aqueous solution. On the other hand, the surface of the Cu plate that was not immersed became entirely black. The field-emission scanning electron microscopy (SEM) image of the Cu plate before the reaction showed a smooth surface (Fig. S2†). Interestingly, nanobelt arrays were densely formed on the surface of the non-immersed portion (Fig. 1C), which was quite different from the rough surface of the immersed portion (Fig. S3B). The crystal structures of the samples were investigated by measuring the X-ray diffraction patterns (XRD). The XRD pattern of the immersed portion only showed the presence of Cu (Fig. S3C,† JCPDS No. 4-836). However, the XRD pattern of the non-immersed portion featured two diffraction patterns attributed to Cu and CuO (JCPDS No. 5-661) (Fig. 1D). Thus, the CuO nanobelt arrays were only formed on the non-immersed portion of the Cu plate by the VO process.

Fig. S4, S5 and S6 show color changes of copper substrates and SEM images and XRD patterns of the non-immersed portion obtained at different reaction periods, respectively.† The only non-immersed portion gradually changed to black, indicating formation of CuO nanoarrays. Tiny thorn-like nanostructures formed on the Cu substrate within 5 min and further heating led to the growth of quasi one-dimensional nanowire arrays (from 5 min to 1 h). These structures did not show any X-ray diffraction peaks besides those attributed to Cu, which indicates that they are amorphous. After 3 h, nanobelt arrays formed and their density increased with increasing reaction time (Fig. S5D–E†). The XRD diffraction pattern of the nanobelts corresponds to the CuO crystal (Fig. S6D–E).† The formation of CuO nanobelt arrays did not require immersion of Cu plate into the reaction media. Instead, the CuO nanobelt structures formed on the underside of the Cu plate as shown in Fig. S7.† This indicates that NH_3 (and/or H_2O_2) vapor was involved in the formation of the CuO nanobelt arrays.

Fig. 2 shows a plausible formation mechanism for CuO nanobelt arrays on a Cu substrate. Water vapor containing NH_3 was generated by heating an NH_3 aqueous solution at 80 °C and then was absorbed onto the surface of the Cu plate. The Cu substrate was oxidized to Cu(II) by the O_2 adsorbed from the gas phase and copper ammine complexes were formed by the reaction of the Cu(II) ion and

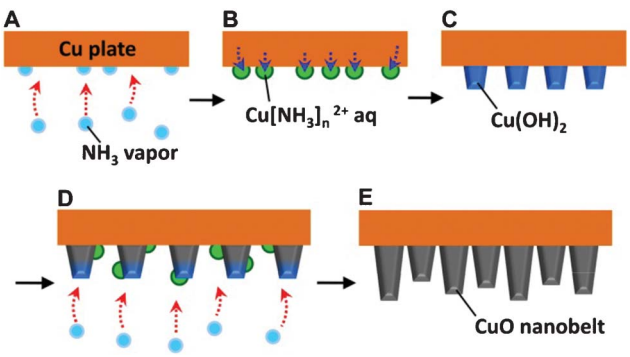

Fig. 2 Plausible formation mechanism of CuO nanobelt arrays by the VO process.

ammonia. Under basic conditions (pH = 11.2), OH^- replaces NH_3 in the $Cu[NH_3]_n^{2+}$ complex giving rise to square planar $Cu(OH)_4^{2-}$ units. It has been reported that $Cu(OH)_2$ nanoribbons preferentially grow along the [100] direction by the assembly of >$Cu(OH)_2$Cu< chains.[21] Accordingly, the $Cu(OH)_2$ nanobelt arrays formed by one-dimensional assembly of the $Cu(OH)_4^{2-}$ units. After further heat treatment at 80 °C, the $Cu(OH)_2$ nanobelt arrays rapidly transformed to CuO. The XRD signals attributed to $Cu(OH)_2$ crystal were not found for all samples which were obtained at varied reaction periods. It has been reported that $Cu(OH)_2$ is a metastable phase which easily transforms into CuO more stable, either in the solid state by a thermal dehydration or at room temperature in aqueous basic solutions.[26] Unfortunately in the present synthetic system, however, observation of metastable $Cu(OH)_2$ is hindered by the rapid transformation process at 80 °C. The growth reactions continuously occurred during the heat treatment, and the perfect CuO nanoarrays were obtained. On the other hand, significant nanostructures were not formed on the immersed portion (Fig. S3†). The amount of copper in the NH_3/H_2O_2 aqueous solutions after the VO reaction was determined by ICP-AES measurements, as shown in Fig. S8.† The cocentration of copper was increased with increasing reaction time. It is assumed that the immersed portion of the Cu substrate was oxidized by dissolved oxygen and soluble copper-amine complexes were formed in the aqueous solution. Thus, nanoarray structures could not be obtained on the immersed portion.

The formation of CuO nanobelt arrays requires the presence of NH_3 vapor. Fig. S9, S10 and S11 show changes in appearance of copper substrates and the SEM images and XRD patterns, respectively, of a Cu plate immersed in an NH_3 aqueous solution at 80 °C.† CuO nanobelt arrays gradually formed on the Cu plate. The addition of H_2O_2 enhances the formation of the CuO nanobelt arrays (Fig. S5A–B *vs.* Fig. S10A–B†). It is assumed that the H_2O_2 molecules are involved in the oxidation process of Cu by supplying O_2 *via* thermal decomposition ($H_2O_2(aq) \rightarrow H_2O + O_2(g)$) and by the following direct redox reaction:[27]

$$Cu = Cu^{2+} + 2e^- \quad +0.340\ V\ \textit{vs.}\ SHE \qquad (1)$$

$$H_2O_2 + 2H^+ + 2e^- = 2H_2O \quad +1.763\ V\ \textit{vs.}\ SHE \qquad (2)$$

The rapid formation of Cu^{2+} in the initial reaction stage increased the rate of CuO nanobelt formation. The pH of the NH_3 aqueous solution also affects the formation of CuO nanobelt structures. Fig. S12 shows SEM images of the Cu plate after the VO process in an NH_3 aqueous solution with different pH values.† At pH 2, the nanobelt structures barely formed; however, the formation density of plate-like nanostructures increased with increasing pH. This indicates that OH^- ions play a critical role in the growth of CuO nanobelts. It is likely that the precursor $Cu(OH)_2$ nanostructures did not form under the low pH conditions.

CuO/metal oxides hetero-composite nanomaterials have also attracted much attention due to their fascinating semiconducting and catalytic properties.[28] A brass plate (Cu–Zn alloy) was partly immersed in a 100 mM NH_3 aqueous solution and the sample was heated at 80 °C for 24 h. The color of the non-immersed portion of the brass plate changed to black indicating the formation of CuO/ZnO nanobelt/nanorod composites (Fig. S13†). It is expected that

various CuO/metal oxide nanoarrays can be obtained from Cu-based alloys using the VO synthetic method.

The electrocatalytic activity of the CuO nanobelt arrays/Cu electrode towards the oxidation of glucose in an alkaline solution was investigated. The cyclic voltammograms (CVs) of the CuO nanobelt arrays/Cu electrode in different concentrations of glucose were measured, as shown in Fig. S14.† In the alkaline solution, a broad reduction with a peak potential of about 0.3 V *vs.* Ag/AgCl was observed. This wave might be attributed to a Cu(II)/Cu(III) redox reaction.[29] Upon addition of glucose, the electrode exhibited significant oxidation of the glucose starting at *ca.* 0.25 V *vs.* Ag/AgCl with a shoulder peak at 0.6 V *vs.* Ag/AgCl; the response was concentration-dependent. Thus, the CuO nanobelt arrays/Cu electrode is electrocatalytically active towards glucose oxidation. This may be attributed to the proposed involvement of Cu(II) and Cu(III) surface species in the oxidation of glucose.[30] Fig. 3 shows a typical amperometric response of the CuO nanobelt/Cu electrode to the successive addition of glucose at an applied potential of 0.6 V *vs.* Ag/AgCl. The CuO/Cu electrode responded to the changes in glucose concentration and shows fast response, *i.e.*, the response reaches 95% of the steady-state value within 2 s. The corresponding calibration curve for the glucose sensor is shown in Fig. 3B. The sensor shows a sensitivity of 582.0 μA mM^{-1} cm^{-2} and a detection limit of less than 1 μM. The performance of the CuO nanobelt sensor was compared with other nonenzymatic glucose sensors, as shown in Table S1.† The sensitivity and detection limit of the CuO nanobelt/Cu electrode are higher and lower, respectively, than those of the other glucose sensors. This is partly due to the direct deposition of CuO nanocrystals onto the Cu plate with high electrical conductivity *via* the VO process. The good electrochemical ability and simple, one-pot, rapid, low-temperature fabrication would make the as-prepared CuO nanobelt arrays/Cu electrode an excellent sensing platform for various chemicals such as H_2S,[31] CO,[32] and volatile organic compounds.[33]

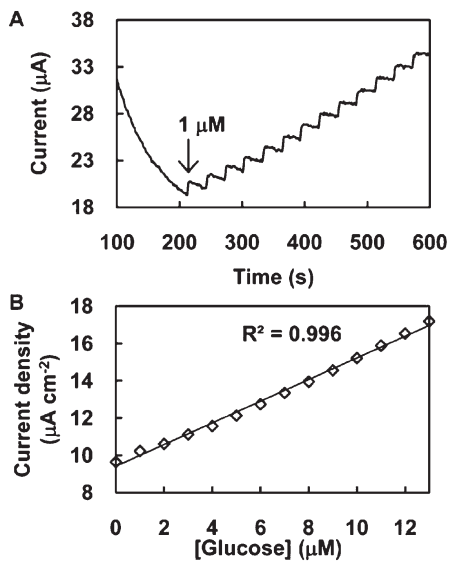

Fig. 3 (A) CA response of CuO nanobelt arrays/Cu plate electrode at 0.6 V upon the addition of glucose solution to a 0.1 M NaOH aqueous solution. (B) Corresponding calibration curve (current density *versus* glucose concentration).

Conclusions

In conclusion, CuO nanobelts and CuO/ZnO composite nanoarrays were successfully obtained by a one-pot, low-temperature, rapid alkaline vapor oxidation method. The resultant CuO nanobelt/Cu nonenzymatic glucose sensor presents attractive analytical features such as a fast response time, high sensitivity, and a low detection limit. We envisage that various CuO/metal oxide composites and other metal oxide nanoarrays with various properties can be obtained by adapting the VO method to other Cu-based alloys and metal plates.

This work was partly supported by a Grant-in-Aid for Young Scientists (B, No. 22710102) from the Ministry of Education, Culture, Sports, Science and Technology, Japan and JST CREST.

References

1 (*a*) J. G. Bendnorz and K. A. Muller, *Z. Phys. B: Condens. Matter*, 1986, **64**, 189; (*b*) M. K. Wu, J. R. Ashburn, C. J. Torng, P. H. Hor, R. L. Meng, L. Gao, Z. J. Huang, Y. Q. Wang and C. W. Chu, *Phys. Rev. Lett.*, 1987, **58**, 908.
2 J. Ziolo, F. Borsa, M. Corti, A. Rigamonti and F. Parmigiani, *J. Appl. Phys.*, 1990, **67**, 5864.
3 C. T. Hsieh, J. M. Chen, H. H. Lin and H. C. Shih, *Appl. Phys. Lett.*, 2003, **83**, 3383.
4 L. Reijnen, B. Meester, A. Goossens and J. Schoonman, *Chem. Vap. Deposition*, 2003, **9**, 15.
5 M. K. Wu, J. R. Ashburn, C. J. Torng, P. H. Hor, R. L. Meng, L. Gao, Z. J. Huang, Y. Q. Wang and C. W. Chu, *Phys. Rev. Lett.*, 1987, **58**, 908.
6 J. Chen, K. Wang, L. Hartman and W. Zhou, *J. Phys. Chem. C*, 2008, **112**, 16017.
7 A. P. L. Batista, H. W. P. Carvalho, G. H. P. Luz, P. F. Q. Martins, M. Gonçalves and L. C. A. Oliveira, *Environ. Chem. Lett.*, 2010, **8**, 63.
8 S. Anandan, X. Wen and S. Yang, *Mater. Chem. Phys.*, 2005, **93**, 35.
9 P. Podhájeckýa, Z. Zábranskýa, P. Nováka, Z. Dobiášováb, R. Černýb and V. Valvodab, *Electrochim. Acta*, 1990, **35**, 245.
10 (*a*) S. Jammi, S. Sakthivel, L. Rout, T. Mukherjee, S. Mandal, R. Mitra, P. Saha and T. Punniyamurthy, *J. Org. Chem.*, 2009, **74**, 1971; (*b*) M. L. Kantam, J. Yadav, S. Laha, B. Sreedhar and S. Jha, *Adv. Synth. Catal.*, 2007, **349**, 1938.
11 (*a*) Y. Liu, Q. Fu and M. F. Stephanopoulos, *Catal. Today*, 2004, **93–95**, 241; (*b*) Y. Feng and X. Zheng, *Nano Lett.*, 2010, **10**, 4762.
12 J. B. Reitz and E. I. Solomon, *J. Am. Chem. Soc.*, 1998, **120**, 11467.
13 L. Xu, S. Sithambaram, Y. Zhang, C.-H. Chen, L. Jin, R. Joesten and S. L. Suib, *Chem. Mater.*, 2009, **21**, 1253.
14 (*a*) Y. Xia, P. Yang, Y. Sun, Y. Wu, B. Mayers, B. Gates, Y. Yin, F. Kim and H. Yan, *Adv. Mater.*, 2003, **15**, 353; (*b*) X. Cao, H. Zeng, M. Wang, X. Xu, M. Fang, S. Ji and L. Zhang, *J. Phys. Chem. C*, 2008, **112**, 5267–5270; (*c*) R. Gao, L. Yin, C. Wang, Y. Qi, N. Lun, L. Zhang, Y.-X. Liu, L. Kang and X. Wang, *J. Phys. Chem. C*, 2009, **113**, 15160; (*d*) Y. Wang, H. Xia, L. Lu and J. Lin, *ACS Nano*, 2010, **4**, 1425; (*e*) W. Liu, Z.-M. Cui, Q. Liu, D.-W. Yan, J.-Y. Wu, H.-J. Yan, Y.-L. Guo, C.-R. Wang, W.-G. Song, Y.-Q. Liu and L.-J. Wan, *J. Am. Chem. Soc.*, 2007, **129**, 12922.
15 M. H. Huang, S. Mao, H. Feick, H. Yan, Y. Wu, H. Kind, E. Weber, R. Russo and P. Yang, *Science*, 2001, **292**, 1897.
16 M. Law, L. E. Greene, J. C. Johnson, R. Saykally and P. Yang, *Nat. Mater.*, 2005, **4**, 455.
17 Y. Li, B. Tan and Y. Wu, *Nano Lett.*, 2008, **8**, 265.
18 Y. Qin, X. Wang and Z. L. Wang, *Nature*, 2008, **451**, 809.
19 L. Qu, L. Dai, M. Stone, Z. Xia and Z. L. Wang, *Science*, 2008, **322**, 238.
20 T. Zhao, J. Wu and J. Huang, *J. Am. Chem. Soc.*, 2009, **131**, 3158.
21 X. Wen, W. Zhang and S. Yang, *Langmuir*, 2003, **19**, 5898.
22 X. Jiang, T. Herricks and Y. Xia, *Nano Lett.*, 2002, **2**, 1333.
23 X. Wen, Y. Xie, C. L. Choi, K. C. Wan, X.-Y. Li and S. Yang, *Langmuir*, 2005, **21**, 4729.
24 J. Liu, X. Huang, Y. Li, K. M. Sulieman, X. He and F. Sun, *J. Mater. Chem.*, 2006, **16**, 4427.
25 X. Yang, J. Zhuang, X. Li, D. Chen, G. Ouyang, Z. Mao, Y. Han, Z. He, C. Liang, M. Wu and J. C. Yu, *ACS Nano*, 2009, **3**, 1212.
26 Y. Cudennec and A. Lecerf, *Solid State Sci.*, 2003, **5**, 1471–1474.

27 *Handbook of Chemistry: Pure Chemistry*, Maruzen, Tokyo, 5th edn, 2004.
28 (*a*) D. H. Yoon, J. H. Yu and G. M. Choi, *Sens. Actuators, B*, 1998, **46**, 15; (*b*) S.-T. Jun and G. M. Choi, *J. Am. Ceram. Soc.*, 1998, **81**, 695; (*c*) Y. Zhu, C.-H. Sow, T. Yu, Q. Zhao, P. Li, Z. Shen, D. Yu and J. T.-L. Thong, *Adv. Funct. Mater.*, 2006, **16**, 2415; (*d*) N. Wu, M. Zhao, J.-G. Zheng, C. Jiang, B. Myers, S. Li, M. Chyu and S. X. Mao, *Nanotechnology*, 2005, **16**, 2878; (*e*) H. A. Zaidi and K. K. Pant, *Ind. Eng. Chem. Res.*, 2008, **47**, 2970.
29 (*a*) L. D. Burke, G. M. Bruton and J. A. Collins, *Electrochim. Acta*, 1998, **44**, 1467; (*b*) Z Zhang, X. Su, H. Yuan, Q. Sun, D. Xiao and M. M. F. Choi, *Analyst*, 2008, **133**, 126; (*c*) Q. Xu, Y. Zhao, J. Z. Xu and J.-J. Zhu, *Sens. Actuators, B*, 2006, **114**, 379.
30 X. Kang, Z. Mai, X. Zou, P. Cai and J. Mo, *Anal. Biochem.*, 2007, **363**, 143.
31 J. Chen, K. Wang, L. Hartman and W. Zhou, *J. Phys. Chem. C*, 2008, **112**, 16017.
32 J. H. Yu and G. M. Choi, *Sens. Actuators, B*, 2001, **75**, 56.
33 D. Barreca, E. Comini, A. Gasparotto, C. Maccato, C. Sada, G. Sberveglieri and E. Tondello, *Sens. Actuators, B*, 2009, **141**, 270.

